Am J Physiol Cell Physiol 283: C792–C801, 2002.
First published May 15, 2002; 10.1152/ajpcell.00425.2001.

Stiffness changes in cultured airway smooth muscle cells

STEVEN S. AN, RACHEL E. LAUDADIO, JEAN LAI,
RICK A. ROGERS, AND JEFFREY J. FREDBERG
Physiology Program, Department of Environmental Health, Harvard School of Public Health, Boston, Massachusetts 02115

Received 5 September 2001; accepted in final form 11 May 2002

An, Steven S., Rachel E. Laudadio, Jean Lai, Rick A. Rogers, and Jeffrey J. Fredberg. Stiffness changes in cultured airway smooth muscle cells. *Am J Physiol Cell Physiol* 283: C792–C801, 2002. First published May 15, 2002; 10.1152/ajpcell.00425.2001.—Airway smooth muscle (ASM) cells in culture stiffen when exposed to contractile agonists. Such cell stiffening may reflect activation of the contractile apparatus as well as polymerization of cytoskeletal biopolymers. Here we have assessed the relative contribution of these mechanisms in cultured ASM cells stimulated with serotonin (5-hydroxytryptamine; 5-HT) in the presence or absence of drugs that inhibit either myosin-based contraction or polymerization of filamentous (F) actin. Magnetic twisting cytometry was used to measure cell stiffness, and associated changes in structural organization of actin cytoskeleton were evaluated by confocal microscopy. We found that 5-HT increased cell stiffness in a dose-dependent fashion and also elicited rapid formation of F-actin as marked by increased intensity of FITC-phalloidin staining in these cells. A calmodulin antagonist (W-7), a myosin light chain kinase inhibitor (ML-7) and a myosin ATPase inhibitor (BDM) each ablated the stiffening response but not the F-actin polymerization induced by 5-HT. Agents that inhibited the formation of F-actin (cytochalasin D, latrunculin A, C3 exoenzyme, and Y-27632) attenuated both baseline stiffness and the extent of cell stiffening in response to 5-HT. Together, these data suggest that agonist-evoked stiffening of cultured ASM cells requires actin polymerization as well as myosin activation and that neither actin polymerization nor myosin activation by itself is sufficient to account for the cell stiffening response.

cell mechanics; cytoskeleton; actin microfilaments; myosin; serotonin

AIRWAY SMOOTH MUSCLE (ASM) is the key end effector of acute airway narrowing in asthma. Studies of the contractile behavior of ASM have relied largely on the use of tissue strip preparations or freshly dissociated smooth muscle cells (6, 8, 12, 45). More recently, however, it was demonstrated that the ASM cell passaged in culture represents a useful model system because it retains important functional responses to agonists and signaling pathways implicated in asthma (5, 16, 24, 30, 35). Using magnetic twisting cytometry (MTC), Hubmayr et al. (16) showed that cultured ASM cells stiffen when challenged with a panel of contractile agonists reported to increase intracellular Ca^{2+} concentration ($[Ca^{2+}]_i$) or inositol 1,4,5-trisphosphate (IP_3) formation and that the extent of cell stiffening rank orders with the relative potency of these same agonists in mediating bronchoconstriction at the level of isolated muscle strips (1, 9). Conversely, cell stiffness decreases progressively with increasing doses of bronchodilating agonists that are known to increase intracellular cAMP and cGMP levels (16, 35). These findings provide evidence of pharmacomechanical coupling in ASM cells passaged in culture, but the underlying mechanism responsible for stiffening in these cells is unclear.

Agonist-evoked cell stiffening in cultured ASM cells may be attributable in part to activation of the contractile apparatus, thereby reflecting actomyosin-based contraction. Phosphorylation of the 20,000-dalton myosin light chain (LC_{20}) is the central regulatory mechanism of smooth muscle contraction. When phosphorylated by Ca^{2+}/calmodulin-dependent myosin light chain kinase, LC_{20} promotes actin-activated myosin motor activity and tension generation (19, 36). Accordingly, the mechanical stiffening of adherent ASM cells, as measured by MTC, may reflect receptor-coupled activation of myosin phosphorylation, resulting in the cyclic interaction between myosin cross bridges and the actin lattice (11, 19).

Additionally, some part of the observed cell stiffening might be attributable to the agonist-induced formation, remodeling, and reorganization of noncontractile elements of the cytoskeleton (CSK). Gunst and colleagues (10, 27, 32, 44) demonstrated that contractile agonists, in addition to triggering actomyosin-based force generation, cause polymerization of filamentous (F) actin as well as phosphorylation of the CSK proteins paxillin and talin that are localized to the membrane-associated dense-plaque sites of smooth muscle cells. These observations led to the suggestion that dynamic changes in the actin CSK and its attachment to the cell membrane may be an important component of force generation in ASM (7, 27, 40).

Address for reprint requests and other correspondence: S. S. An, Physiology Program, Harvard School of Public Health, 665 Huntington Ave., Bldg. I, Rm. 1308, Boston, MA 02115 (E-mail: san@hsph.harvard.edu).

The costs of publication of this article were defrayed in part by the payment of page charges. The article must therefore be hereby marked "*advertisement*" in accordance with 18 U.S.C. Section 1734 solely to indicate this fact.

The present study was undertaken to assess the relative contribution of myosin motors vs. changes in the actin CSK during agonist-evoked mechanical stiffening of cultured ASM cells. Using MTC, we measured the stiffness of cultured rat ASM cells exposed to serotonin (5-hydroxytryptamine; 5-HT), which was shown previously to increase $[Ca^{2+}]_i$ (39) and cause acute airway narrowing in the rat (31). To assess the contribution of myosin activation to the cell stiffening induced by 5-HT, we used a panel of inhibitors, each of which acts via a distinct mode of action to block the catalytic activity of myosin: the calmodulin antagonist *N*-(6-aminohexyl)-5-chloro-1-naphthalenesulfonamide (W-7), the myosin light chain kinase inhibitor 1-(5-iodonaphthalene-1-sulfonyl)-1*H*-hexahydro-1,4-diazepine (ML-7), and the myosin ATPase inhibitor 2,3-butanedione 2-monoxime (BDM). To assess the relative contribution of F-actin polymerization to the increase in cell stiffness, we used a panel of inhibitors that are known to block the formation of F-actin: cytochalasin D, latrunculin A, *Clostridium botulinum* C3 exoenzyme, and Y-27632. With each of these inhibitors, we also evaluated structural changes in the actin CSK with confocal microscopy.

MATERIALS AND METHODS

Cell isolation and culture. Rat ASM cells were prepared as previously described (39). Ten- to twelve-week-old female Sprague-Dawley rats (Harlan; Indianapolis, IN) were intraperitoneally injected with pentobarbital sodium (35 mg/kg), and the tracheas were aseptically excised and placed in Ca^{2+},Mg^{2+}-free Hanks' balanced salt solution (HBSS) of the following composition (mM): 5 KCl, 0.3 KH_2PO_4, 138 NaCl, 4 $NaHCO_3$, 0.3 Na_2HPO_4, and 1.0 glucose. The isolated tracheas were cleaned of connective tissues, cut longitudinally through the cartilage, and enzymatically dissociated with HBSS containing 0.05% elastase type IV and 0.2% collagenase type IV for 30 min in a shaking water bath at 37°C. Dissociated cells in suspension were centrifuged and resuspended in Dulbecco's modified Eagle's medium (DMEM)-Ham's F-12 medium (1:1 vol/vol) supplemented with 10% fetal bovine serum (FBS) and antibiotics (100 U/ml penicillin, 100 μg/ml streptomycin, and 2.5 μg/ml amphotericin-β). Cells were plated on culture flasks and grew until confluence at 37°C in humidified air containing 5% CO_2. The medium was changed every 3–4 days, and confluent cells were passaged with 0.25% trypsin-0.02% EDTA solution every 10–14 days. ASM cells in culture were elongated and spindle shaped, grew with the typical hill-and-valley appearance, and showed positive staining for the smooth muscle-specific proteins α-actin and calponin.

Magnetic twisting cytometry. Mechanical properties of cultured rat ASM cells were measured with MTC as previously described (41). In brief, serum-deprived cells adherent on collagen-coated wells (500 ng/cm^2) were incubated for 20 min with $\sim 5 \times 10^4$ ferrimagnetic beads (4.5 μm in diameter) coated with synthetic Arg-Gly-Asp (RGD) containing peptides (50 μg peptide/mg beads) in serum-free medium containing 1% BSA. This allowed a specific binding of the beads to cell surface integrin receptors on adherent cells. Unbound beads were removed by washing cells with serum-free medium. The wells were then individually placed within the magnetometer and maintained at 37°C.

The beads were first magnetized with a brief 1,000-G pulse so that their magnetic moments were aligned in one direction, parallel to the surface on which cells were plated. Subsequently, an external magnetic "twisting" field (26 G) was applied orthogonal to the original field, yielding a magnetic torque of 80 dyn/cm^2. This second twisting magnetic field was too weak to remagnetize the beads and instead caused the bead to rotate, as would a compass needle, to reorient the magnetic moment toward alignment with the applied field. The magnetometer measured changes in the component of the remnant magnetic field generated by the beads in the original direction. From these data, the ratio of specific torque to bead rotation was computed and expressed as the apparent cell stiffness (41).

Confocal laser scanning microscopy. We used a modification of the methods used by Togashi et al. (38) to visualize actin stress fibers within rat ASM cells passaged in culture. First, we aseptically inserted glass coverslips (12-mm diameter) into 24-well tissue culture flask and coated them with collagen at a concentration of 500 ng/well. On the day of the experiment, serum-deprived cells were seeded at 100,000 cells to each well.

After each experimental protocol (see *Experimental protocols*), adherent ASM cells were fixed in 3.7% paraformaldehyde-phosphate buffered saline (PBS) containing 0.1% Triton X-100 for 10 min at room temperature (pH 7.2). Cells were then washed twice with PBS and subsequently permeabilized with 0.2% Triton X-100 in PBS for 10 min. Incubation and washing were performed in parallel for all wells. To localize F-actin, cells were stained with fluorescein isothiocyanate (FITC)-labeled phalloidin (5 μg/ml) in blocking solution (1% BSA-0.1% Triton X-100 in PBS) overnight in a dark room at room temperature. The next day, cells were extensively washed with PBS and each coverslip was mounted on a slide with a mounting medium (Gel/Mount; Biomeda).

FITC-labeled phalloidin staining of F-actin was visualized with a Leica TCSNT confocal laser scanning microscope (Leica, Exton, PA) fitted with air-cooled argon and krypton lasers. The excitation and emission wavelengths for FITC-labeled phalloidin were 488 and 525 nm, respectively. Cells were brought into focus under bright-field conditions, and the field of view was selected at random. For each sample, the plane of focus was maintained at 0.5 μm above the coverslip surface.

F-actin staining intensity within cells was calculated with ImageSpace Software (Molecular Dynamics, Sunnyvale, CA) from nonoverlapping square masks (216 μm^2) applied to at least five cytoplasmic regions of each cell under consideration. Regions containing cell margins or nuclear profiles were not included. To standardize the fluorescence intensity measurements among experiments, the time of image capture, the image intensity gain, the image enhancement, and the image black level were optimally adjusted at the outset and kept constant for all experiments. For each experiment, F-actin staining intensity of at least 10 cells from 10 fields was averaged for a single data point. An increase in F-actin staining intensity indicated an increase in actin reorganization.

Experimental protocols. In the present study, third- to eighth-passage ASM cells at confluence were serum deprived and supplemented with 10 μg/ml insulin, 5.5 μg/ml transferrin, and 6.7 μg/μl sodium selenite for 24–48 h before use. These conditions have been shown to maximize the expression of smooth muscle-specific proteins and restore the contractile phenotype of smooth muscle cells (13, 25, 30, 46). On the day of experiments, serum-deprived cells were harvested and plated at 30,000 cells/cm^2 on plastic wells (96-well Re-

movawell, Immulon II; Dynetech) previously coated with collagen at a concentration of 500 ng/cm^2. This concentration of collagen matrix has been optimized for seeding cultured cells and for assessing cell stiffness (16). Cell stiffness was measured 4–24 h later with MTC as described in *Magnetic twisting cytometry*.

In general, three to four measurements of cell stiffness were made for each well both before and after addition of 5-HT. We used the apparent stiffness, as defined by Wang and colleagues (41), expressed as dynes per square centimeter, and cell stiffening induced by 5-HT was expressed as the percent increase from the initial baseline stiffness (unstimulated cells). To assess the relative contribution of contractile protein activation to cell stiffness, cultured ASM cells were incubated for 1 h with or without drugs that inhibit myosin-based contraction (W-7, ML-7, and BDM). For control, the cells were incubated in serum-free medium containing either 1% dimethyl sulfoxide (DMSO) or 0.1% methanol for the same duration of drug treatments. Cell stiffness was measured both before and after drug treatments and also after the addition of 10^{-5} M 5-HT.

To modulate events leading to the formation of F-actin (15, 38), ASM cells were treated with C3 exoenzyme (RhoA inhibitor), Y-27632 (Rho-kinase inhibitor), cytochalasin D, or latrunculin A. Adherent cells were incubated with or without C3 exoenzyme (final concentration 10 μg/ml) for 24–48 h in DMEM-Ham's F-12 (1:1 vol/vol) medium containing 1% FBS. Subsequently, the cells were reequilibrated in serum-free medium with or without C3 exoenzyme and cell stiffness was measured both before and after addition of 5-HT (10^{-5} M). For Y-27632, cytochalasin D, or latrunculin A, cultured ASM cells were incubated for 1 h with progressively increasing doses of each inhibitor before 5-HT stimulation.

Materials. Tissue culture reagents were obtained from Sigma (St. Louis, MO), with the exception of DMEM-Ham's F-12 (1:1 vol/vol) medium, which was purchased from GIBCO (Grand Island, NY). The synthetic RGD peptide (Peptite 2000; Integra Life Sciences) was provided by Dr. Juerg Tschopp. All drugs were obtained from Sigma, with the exception of *C. botulinum* C3 exoenzyme (RhoA inhibitor) and Y-27632 (Rho-kinase inhibitor), which were purchased from Calbiochem (La Jolla, CA) and Tocris Cookson (Ellisville, MO), respectively. 5-HT and C3 exoenzyme were reconstituted in sterile distilled water. BDM, ML-7, cytochalasin D, latrunculin A, and Y-27632 were prepared in DMSO; W-7 was dissolved in 10% methanol. On the day of the experiments, all reagents were diluted to final concentrations in serum-free medium yielding either 1% DMSO or 0.1% methanol in final volume.

Statistics. Data are presented as means ± SE; n represents the number of experiments. Student's t-test was used for statistical comparison of two means ($P < 0.05$ was considered significant). The correlation between two variables such as stiffness of drug-treated and untreated cells was analyzed by Pearson's correlation analysis ($P < 0.05$ was considered significant).

RESULTS

Contractile state of adherent ASM cells in culture. Rat ASM cells cultured on a collagen-coated surface were stimulated with progressively increasing doses of the contractile agonist 5-HT. Under resting conditions, baseline stiffness of the cells varied from well to well and from day to day (data not shown). Hence, we plotted the extent of cell stiffening induced by different doses of 5-HT as the percent change from the respective baseline stiffness (Fig. 1). Cell stiffness increased in a dose-dependent manner and reached a plateau at 10^{-6} M 5-HT. The mean stiffness in unstimulated ASM cells was 99.10 ± 7.53 dyn/cm^2 at baseline and then increased to 142.67 ± 8.47 dyn/cm^2 in response to 5-HT (10^{-5} M).

Cell stiffness increased somewhat after a 1-h incubation with serum-free medium (ITS) or serum-free medium containing 1% DMSO but less so with serum-free medium containing 0.1% methanol (Fig. 2). Nevertheless, in response to 5-HT (10^{-5} M), cell stiffness further increased above baseline stiffness by 84.1 ± 16.8% for ITS, 61.5 ± 11.5% for 1% DMSO, or 56.6 ± 10.2% for 0.1% methanol-treated cells (Fig. 2). There was no statistical difference between these changes.

Role of contractile machinery within cultured ASM cells. 5-HT acts via the 5-HT$_{2c}$-like receptors coupled to phospholipase C and elicits the mobilization of $[Ca^{2+}]_i$ in cultured rat ASM cells (33, 39). An increase in $[Ca^{2+}]_i$ initiates smooth muscle contraction via binding to calmodulin, which then activates myosin light chain kinase (19). To assess whether cell stiffening induced by 5-HT is attributable to activation of the calmodulin-dependent signaling pathways, ASM cells were incubated for 1 h with serum-free medium containing 0, 1, 10, 20, 50, or 100 μM W-7 before 5-HT (10^{-5} M) stimulation. For control, the cells were incubated for 1 h with 0.1% methanol (medium used to prepare working concentrations of W-7).

Cells treated with W-7 exhibited a dose-dependent reduction of cell stiffening induced by 5-HT (Fig. 3). At high concentrations, a 1-h incubation with W-7 decreased cell stiffness below initial baseline and prevented any further increase in cell stiffness induced by 5-HT. The concentration of W-7 that caused a decrease in cell stiffness equal to 50% of the 5-HT response in the absence of W-7 (IC_{50}) was ~16 μM.

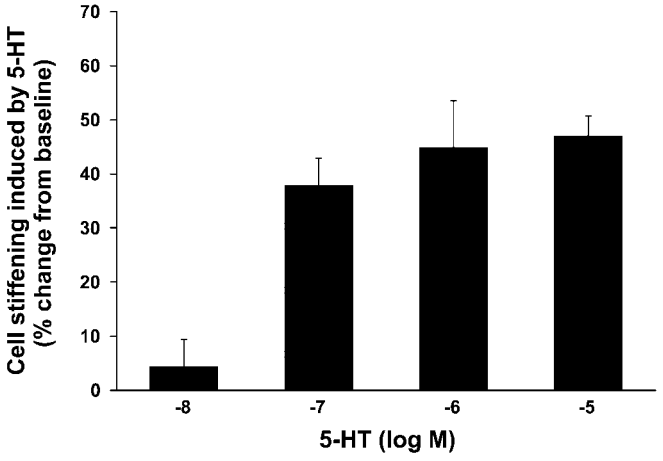

Fig. 1. Stiffness changes in response to serotonin (5-hydroxytryptamine; 5-HT). Airway smooth muscle (ASM) cells cultured on a collagen-coated surface were stimulated with increasing doses of 5-HT. Cell stiffening induced by 5-HT (10^{-8}–10^{-5} M) was plotted as the % change from respective baseline stiffness. Data are presented as means ± SE (n = 6–17 wells).

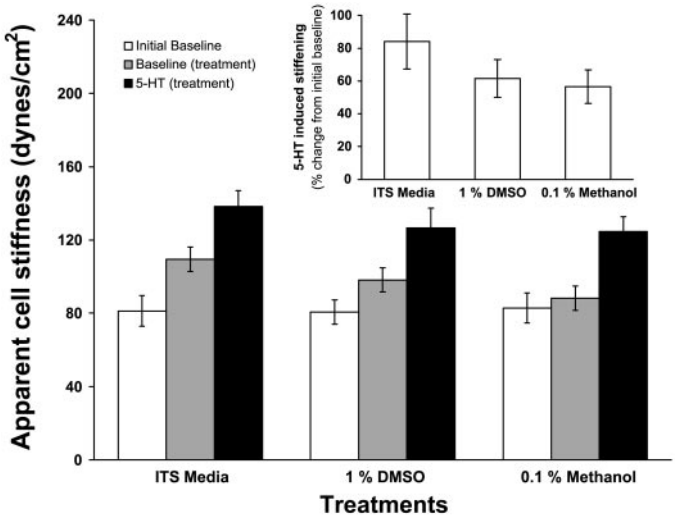

Fig. 2. The contractile state of ASM cells is not affected by treatments with 1% dimethyl sulfoxide (DMSO) or 0.1% methanol. ASM cells were incubated for 1 h with serum-free medium (ITS), 1% DMSO, or 0.1% methanol before 5-HT stimulation. Open bars, initial baseline stiffness before the treatment; gray bars, apparent stiffness after 1-h incubation with the treatment; black bars, apparent stiffness induced by 5-HT. *Inset*: for each condition, cell stiffening induced by 5-HT (10^{-5} M) is expressed as the % change from respective baseline stiffness. Data are presented as means ± SE (n = 10–13 wells).

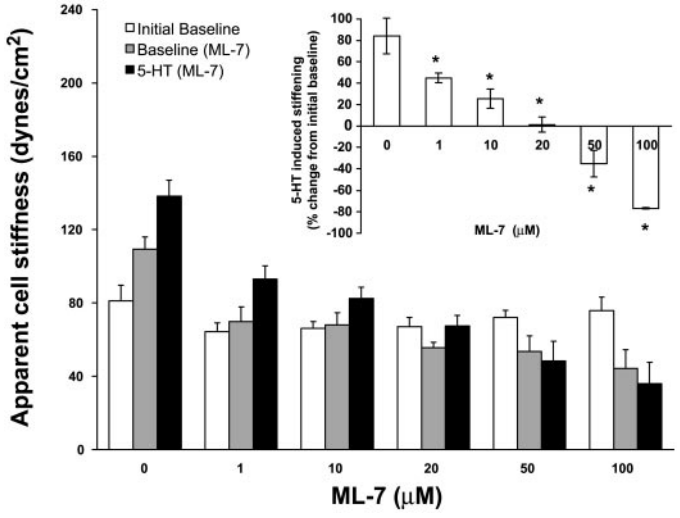

Fig. 4. ML-7 ablates the contractile response to 5-HT. ASM cells were incubated for 1 h with 0, 1, 10, 20, 50, or 100 μM ML-7 before 5-HT stimulation. Open bars, initial baseline stiffness; gray bars, apparent stiffness after a 1-h incubation with ML-7; black bars, apparent stiffness after addition of 5-HT. *Inset*: cell stiffening induced by 5-HT (10^{-5} M) is expressed as the % change from respective baseline stiffness. *Significant difference from cells incubated with 0 μM ML-7. Data are presented as means ± SE (n = 3–13 wells).

Cultured ASM cells were also incubated with graded doses of the myosin inhibitors ML-7 and BDM. For control, the cells were treated with serum-free medium containing 1% DMSO (medium used to reconstitute ML-7 and BDM). ASM cells treated for 1 h with ML-7 or BDM exhibited a dose-dependent reduction of both baseline stiffness and cell stiffening induced by 5-HT (Figs. 4 and 5). As shown in Fig. 4, the stiffening response was significantly reduced ($P < 0.05$) in all ML-7-treated cells compared with that of the untreated cells. Likewise, BDM significantly depressed ($P < 0.05$) cell stiffening induced by 5-HT at concentrations of 20 and 50 mM (Fig. 5). The IC_{50} values for ML-7 and BDM were ~3 μM and 17 mM, respectively. At high concentrations, a 1-h incubation with either ML-7 or BDM decreased cell stiffness below initial baseline and prevented any further increase in cell stiffness with 5-HT.

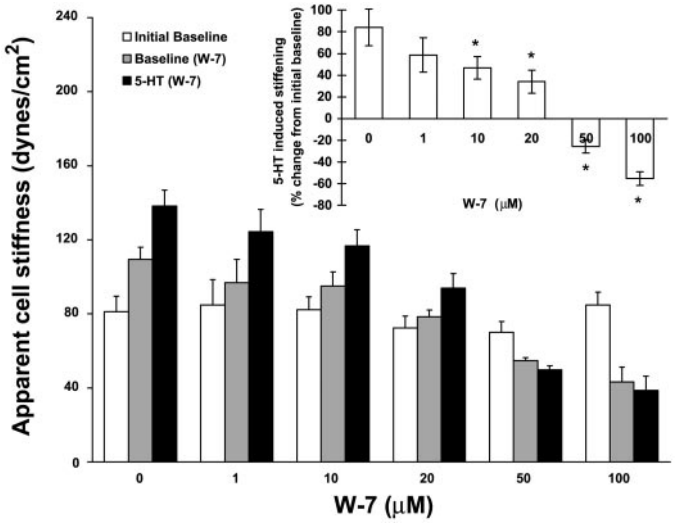

Fig. 3. W-7 ablates the contractile response to 5-HT. ASM cells were incubated for 1 h with 0, 1, 10, 20, 50, or 100 μM W-7 before 5-HT stimulation. Open bars, initial baseline stiffness; gray bars, apparent stiffness after a 1-h incubation with W-7; black bars, apparent stiffness after addition of 5-HT. *Inset*: cell stiffening induced by 5-HT (10^{-5} M) is expressed as the % change from respective baseline stiffness. *Significant difference from cells incubated with 0 μM W-7. Data are presented as means ± SE (n = 5–13 wells).

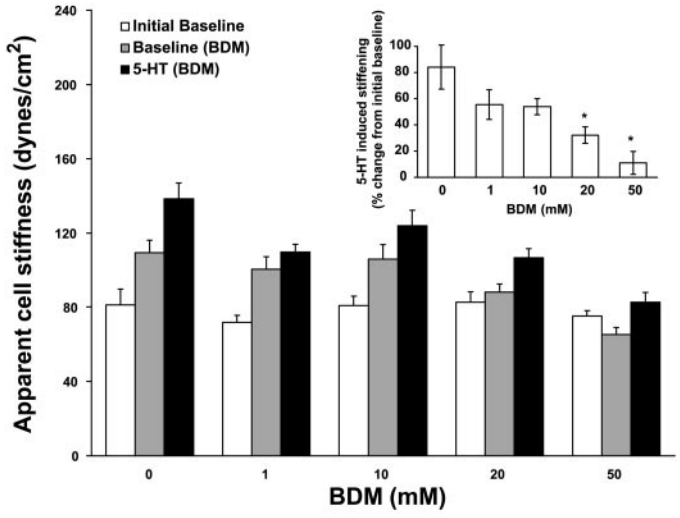

Fig. 5. BDM ablates the contractile response to 5-HT. ASM cells were incubated with 0, 1, 10, 20, or 50 mM BDM before 5-HT stimulation. Open bars, initial baseline stiffness; gray bars, apparent stiffness after a 1-h incubation with BDM; black bars, apparent stiffness after addition of 5-HT. *Inset*: cell stiffening induced by 5-HT (10^{-5} M) is expressed as the % change from respective baseline stiffness. *Significant difference from cells incubated with 0 mM BDM. Data are presented as means ± SE (n = 4–13 wells).

Role of F-actin polymerization within cultured ASM cells. Previous studies demonstrated that contractile agonists modulate the dynamics of the actin CSK within cultured ASM cells by converting G-actin to F-actin (15, 38). An increase in F-actin polymerization is an indication of actin CSK reorganization. Thus cell stiffening evoked by 5-HT may be mediated in part by the formation, remodeling, and reorganization of noncontractile elements within cultured rat ASM cells. To assess that possibility, we used confocal microscopy to examine structural changes in the actin CSK in response to 5-HT stimulation and also to evaluate the effects, if any, of W-7, ML-7, and BDM on the actin-based CSK assembly.

In untreated cells (control), actin microfilaments were visible in the resting condition (unstimulated FITC-phalloidin staining of F-actin in cultured rat ASM cells; Fig. 6*a*). A 5-min exposure to 5-HT (10^{-5} M) elicited further polymerization of actin microfilaments as marked by an increase in the average pixel intensity of FITC-phalloidin staining of F-actin (Fig. 6*b*). The average pixel intensity (scale 0–255) of unstimulated ASM cells was 64.3 ± 9.1 and then increased to 81.8 ± 11.5 in response to 5-HT, representing a 31.4 ± 9.4% increase in pixel intensity (Table 1). For the cells treated with 1% DMSO, the intensity of F-actin staining increased 60.4 ± 25.7% when exposed to 5-HT (Fig. 6, *c* and *d*; Table 1).

ASM cells treated for 1 h with various doses of W-7, ML-7, or BDM did not show noticeable changes in the pixel intensity of F-actin staining compared with that of the unstimulated control cells, except for a 1-h incubation with 50 μM W-7 (Fig. 6, *g*, *i*, and *k*; Table 1). On 5-HT stimulation, FITC-phalloidin staining intensity of F-actin in these cells increased from their respective resting conditions (Fig. 6, *g–l*; Table 1). These myosin inhibitors, at doses that substantially ablated cell stiffening induced by 5-HT, did not block the formation of F-actin, however.

Role of F-actin polymerization in cell stiffness. To assess the relative contribution of F-actin polymerization to cell stiffness, we used direct actin-disrupting agents (cytochalasin D and latrunculin A) as well as inhibitors of Rho activation pathways (C3 exoenzyme and Y-27632). ASM cells treated for 1 h with 1 μM cytochalasin D showed fewer actin microfilaments compared with unstimulated control cells and exhibited a complete ablation of F-actin polymerization induced by 5-HT (Fig. 6, *e* and *f*; Table 1). Likewise, cells treated with latrunculin A (1 μM), C3 exoenzyme (10 μg/ml), or Y-27632 (50 μM) showed significant decreases in the FITC-phalloidin staining intensity of F-actin compared with unstimulated control cells; furthermore, at these same doses, each of the inhibitors completely ablated F-actin polymerization induced by 5-HT (data not shown).

At 1 μM, cytochalasin D caused baseline stiffness to fall but did not completely block the stiffening induced by 5-HT (Fig. 7). Importantly, cytochalasin D at this concentration completely ablated F-actin polymerization. At 10 μM, cytochalasin D caused baseline stiffness to decrease substantially and completely ablated the stiffening induced by 5-HT. ASM cells treated with 1 μM latrunculin A exhibited a decrease in baseline stiffness and complete ablation of the cell stiffening response to 5-HT (Fig. 8). In contrast, cells treated for 24 h with C3 exoenzyme showed only moderate changes in stiffness and cell stiffening induced by 5-HT compared with control cells (Fig. 9). A 48-h incubation with C3 exoenzyme attenuated both baseline cell stiffness and the extent of cell stiffening induced by 5-HT, however. ASM cells treated for 1 h with Y-27632 exhibited a dose-dependent decrease in the extent of cell stiffening induced by 5-HT (Fig. 10). These inhibitors, at doses that completely blocked F-actin polymerization, did not ablate the cell stiffening response to 5-HT, however.

DISCUSSION

ASM cells exposed to the contractile agonist 5-HT increased both cell stiffness and FITC-phalloidin staining of F-actin, thus confirming the findings of others (15, 27, 38). When these cells were pretreated with a panel of myosin inhibitors, however, the cell stiffening induced by 5-HT was largely ablated but F-actin polymerization was not. When cells were pretreated with inhibitors of F-actin polymerization, the cell stiffening induced by 5-HT was substantially attenuated. These results suggest that agonist-evoked cell stiffening requires actin polymerization as well as myosin activation and that neither actin polymerization nor myosin activation by itself is sufficient to account for the observed cell stiffening. In the discussion that follows we begin by pointing out the limitations of the methods that we have used and then go on to discuss the principal findings of this report and their biological implications.

As a model system we used the rat ASM cell in *passages 3–8*. A fundamental limitation of this approach is that the ASM cell can dedifferentiate in culture and tend toward a synthetic rather than a contractile phenotype (14). Panettieri et al. (30) showed, however, that nontransformed human ASM cells that are grown to confluence retain the expression of smooth muscle-specific contractile proteins (α- and γ-actin), although not as much as freshly dissociated cells. Others have reported that prolonged serum deprivation of postconfluent ASM cells further enhances the expression of contractile and regulatory proteins (myosin heavy chain and myosin light chain kinase), which can reach levels that are comparable to those in freshly dissociated cells (13, 25, 46). These cells retain physiological responsiveness, including cytosolic Ca^{2+} release and cAMP production, in response to histamine, leukotrienes, bradykinin, platelet-activating factor, substance P, thromboxane analogs, and isoproterenol (30). Using MTC, Hubmayr et al. (16) demonstrated that human ASM cells in culture stiffen when challenged with a panel of contractile agonists reported to increase $[Ca^{2+}]_i$ or IP_3 formation, whereas cell stiffness decreases progres-

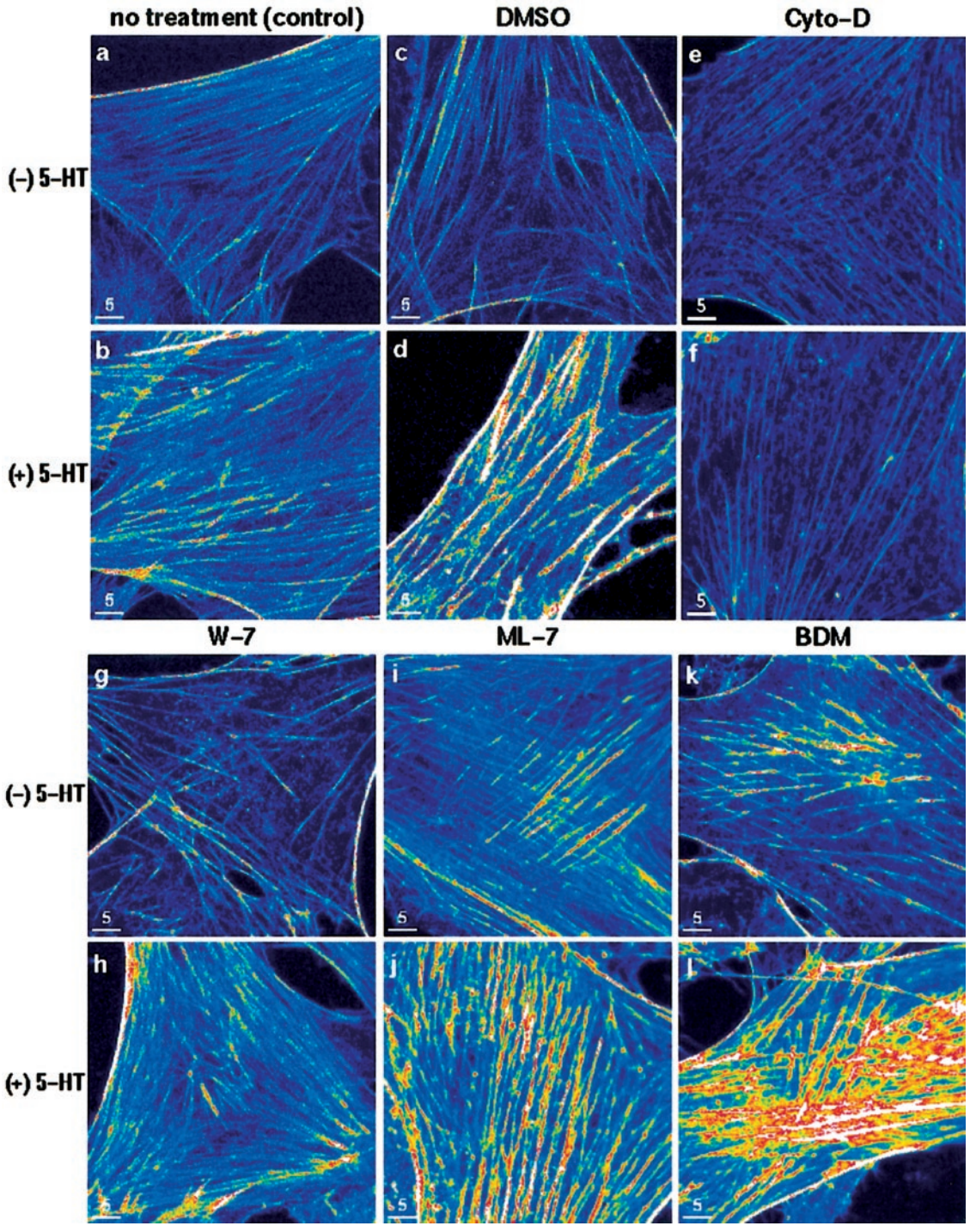

Fig. 6. Representative images from 4 experiments demonstrating that myosin inhibitors do not ablate the F-actin polymerization induced by 5-HT. ASM cells were treated for 1 h without (*a* and *b*) or with DMSO (1%, *c* and *d*), W-7 (30 μM, *g* and *h*), ML-7 (20 μM, *i* and *j*), BDM (20 mM, *k* and *l*), or cytochalasin D (1 μM, *e* and *f*) before a 5-min exposure to 5-HT (10^{-5} M). For each condition, actin cytoskeleton (CSK) was stained with fluorescein isothiocyanate (FITC)-labeled phalloidin and examined by confocal microscopy. (−)5-HT, unstimulated cells; (+)5-HT, cells stimulated with 5-HT. Bar, 5 μm.

sively with increasing doses of bronchodilating agonists known to increase intracellular cAMP and cGMP levels. Shore and colleagues (16, 29, 35) showed that these cells maintain functional coupling to β-adrenergic receptors over many population doublings. We found in the cultured rat ASM cells that 5-HT increased stiffness in a dose-dependent fashion and caused a maximal response (84 ± 17% increase above baseline) at 10^{-5} M. These changes are consistent with previous findings from MTC in human ASM cells (5, 16, 35).

Table 1. *Fluorescence intensity of F-actin staining by FITC-phalloidin in cultured rat ASM cells*

Treatments	Unstimulated	5-HT (10^{-5} M)	% Increase
Control	64.3 ± 9.1	81.8 ± 11.5	31.4 ± 9.4
1 % DMSO	58.2 ± 7.7	94.2 ± 23.5	60.4 ± 25.7
1 μM Cyto-D	50.6 ± 0.9	46.0 ± 0.8	−9.4 ± 4.7
30 μM W-7	62.0 ± 15.3	79.9 ± 20.8	28.1 ± 9.1
50 μM W-7	42.3 ± 10.1	67.8 ± 1.7	80.6 ± 44.7
20 μM ML-7	64.5 ± 16.4	76.9 ± 19.7	18.9 ± 3.4
50 μM ML-7	60.3 ± 12.6	72.1 ± 11.9	20.7 ± 5.5
20 mM BDM	62.2 ± 11.8	97.3 ± 22.4	50.7 ± 13.1
50 mM BDM	62.8 ± 13.6	98.7 ± 22.7	53.3 ± 10.6

Values are mean ± SE pixel intensities (scale 0–255) for n = 4–6 experiments. Airway smooth muscle (ASM) cells were treated for 1 h with or without dimethyl sulfoxide (DMSO; 1%), cytochalasin-D (Cyto-D; 1 μM), W-7 (30–50 μM), ML-7 (20–50 μM), or BDM (20–50 mM) before a 5-min exposure to serotonin (5-HT; 10^{-5} M). For each experiment, at least 10 cells per treatment group were considered, and intensity of F-actin staining was calculated from nonoverlapping square masks (216 μm^2) applied to at least 5 cytoplasmic regions of each cell under consideration. The F-actin polymerization induced by 5-HT is also expressed as the % change from the respective unstimulated conditions.

As a mechanical system, actin filaments formed during adhesion of cells to a substrate in culture may differ significantly from actin filaments present in differentiated smooth muscle tissues; they are bundled into stress fibers oriented to support substrate adhesion rather than tension development and may differ biochemically from the composition of the contractile system of differentiated tissues (10, 20, 21). The active stress generated by these cells in culture can be measured directly by traction microscopy, and it approaches 2 kPa (43); not surprisingly, this corresponds to only a small fraction of the maximum active stress that can be attained at the level of intact isolated contractile tissues, which approaches ~4 kPa in rat aortic strips (2), 20 kPa in guinea pig tracheal smooth muscle (4), and 150 kPa in bovine tracheal smooth muscle (12). Although the level of active stress in the human ASM cell passaged in culture and serum deprived for 24 h is relatively small, this system displays a brisk mechanical response to contractile challenge (5, 16, 26), and induced stiffness changes can be manipulated through an appreciable range; using a more sensitive bead-twisting technique than the one we have used here, Fabry et al. (5) reported changes in cell

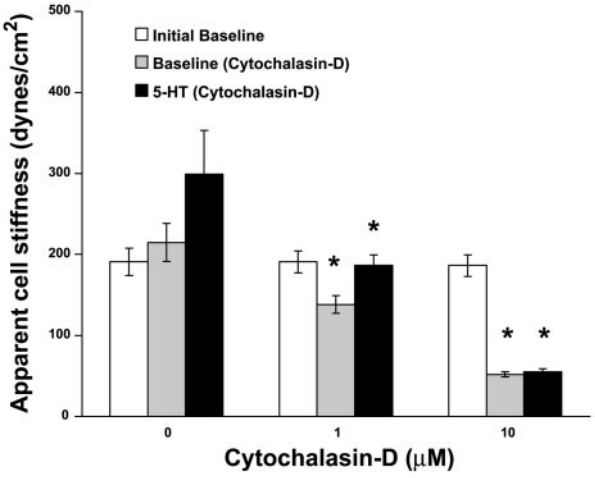

Fig. 7. Cytochalasin D ablates the contractile response to 5-HT. ASM cells were incubated for 1 h with 0, 1, or 10 μM cytochalasin D before 5-HT stimulation. Open bars, initial baseline stiffness; gray bars, apparent stiffness after a 1-h incubation with cytochalasin D; black bars, apparent stiffness induced by 5-HT. *Significant difference from the corresponding treatment of the control. Data are presented as means ± SE (n = 14–15 wells).

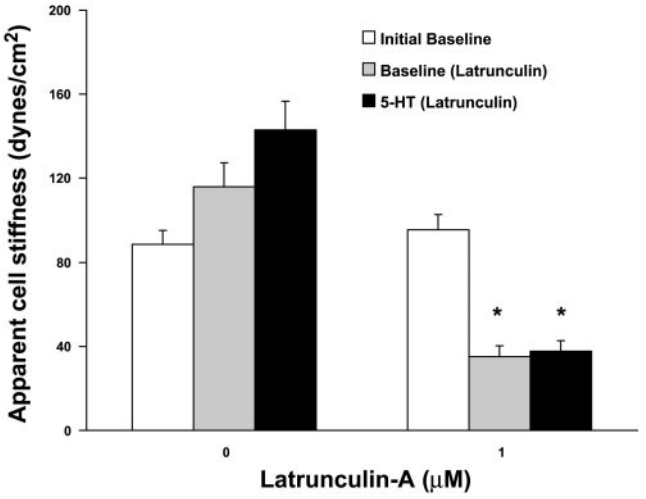

Fig. 8. Latrunculin A ablates the contractile response to 5-HT. ASM cells were incubated for 1 h with or without 1 μM latrunculin A before 5-HT stimulation. Open bars, initial baseline stiffness; gray bars, apparent stiffness after a 1-h incubation with latrunculin A; black bars, apparent stiffness induced by 5-HT. *Significant difference from the corresponding treatment of the control. Data are presented as means ± SE (n = 19 wells).

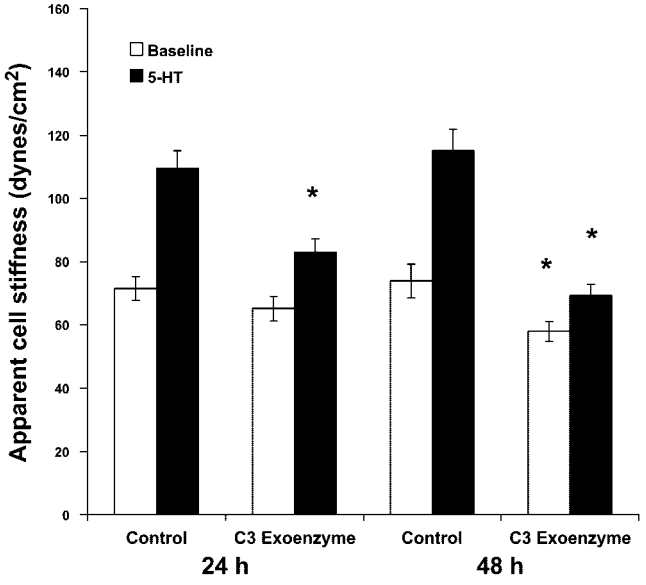

Fig. 9. *Clostridium botulinum* C3 exoenzyme attenuates the contractile response to 5-HT. ASM cells were incubated for 24 or 48 h with or without 10 μg/ml C3 exoenzyme before 5-HT stimulation. Open bars, baseline stiffness; black bars, apparent stiffness induced by 5-HT. *Significant difference from control cells. Data are presented as means ± SE (n = 27 wells).

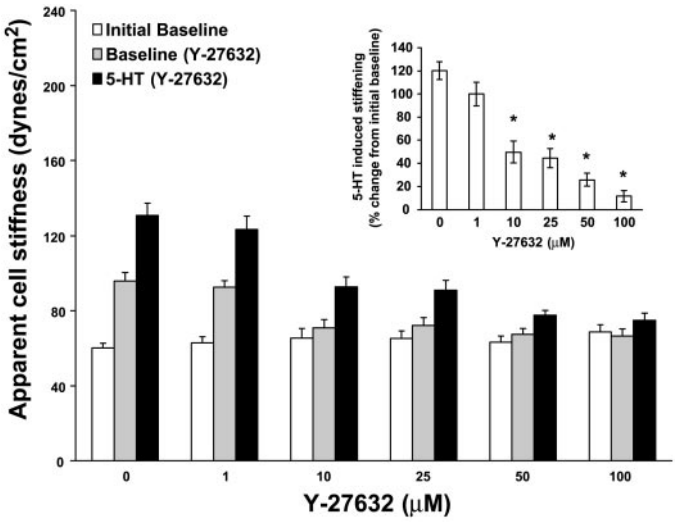

Fig. 10. Y-27632 attenuates the contractile response to 5-HT. ASM cells were incubated for 1 h with 0, 1, 10, 25, 50, or 100 μM Y-27632 before 5-HT stimulation. Open bars, initial baseline stiffness; gray bars, apparent stiffness after a 1-h incubation with Y-27632; black bars, apparent stiffness induced by 5-HT. *Inset*: cell stiffening induced by 5-HT (10^{-5} M) is expressed as the % change from respective baseline stiffness. *Significant difference from cells incubated with 0 μM Y-27632. Data are presented as means ± SE (n = 19 wells).

stiffness of more than sevenfold from maximally relaxed to maximally activated states and showed that the time course of changes in hysteresivity matches well those observed at the level of isolated muscle strips (6). Active stresses measured by traction microscopy span a similarly wide range and closely track changes in CSK stiffness (3, 42, 43), suggesting that changes of CSK stiffness are a reasonable proxy for active force development. Together, observations in ASM cells in intact tissues vs. those passaged in culture suggest that discrepancies of mechanical responses appear to be mostly differences in amount rather than kind. To the extent that this is so, passaged ASM cells in culture may represent an interesting model of the signaling and mechanical events that occur during airway smooth muscle contraction. Nonetheless, the inability of these cells to develop active stresses approaching levels observed in intact tissues may represent a fundamental limitation.

With these limitations in mind, we turn to the question of what factors might account for the induced changes in cell mechanics reported here. Recent studies demonstrated that contractile activation, in addition to eliciting actomyosin-based force generation, also regulates phosphorylation of dense plaque-associated proteins (paxillin, talin, and focal adhesion kinase) and polymerization of actin microfilaments (27, 44). In cultured ASM cells, Hirshman and coworkers (15, 38) reported actin reorganization, as reflected by the conversion of G-actin to F-actin, in response to contractile activation. Mehta and Gunst (27) showed that the inhibition of actin polymerization markedly depresses force development in response to contractile activation without much effect on myosin phosphorylation. In bovine tracheal smooth muscle, Tseng et al. (40) demonstrated that cytochalasin B attenuates carbachol-evoked $[Ca^{2+}]_i$, myosin phosphorylation, and force development. Although cell stiffening and active force generation are usually thought of in the context of myosin activation (16), these findings led Mehta and Gunst to suggest that mechanical changes in ASM cells might be attributable in large part to agonist-induced regulation of actin CSK assembly.

To quantify changes in stress fibers and reorganization of the actin CSK, studies have often used dual-fluorescence labeling with FITC-phalloidin and Texas red DNase I, which provides the relative amounts and configuration of F- and G-actin, respectively (15, 38). In the present study, we chose to quantify the absolute rather than relative changes in F-actin polymerization at and near the dense-plaque sites of ASM cells with confocal microscopy. We found that 5-HT caused rapid formation of actin microfilaments and increased the intensity of FITC-phalloidin staining of F-actin. Our findings are in agreement with earlier reports that the actin CSK is dynamically regulated during muscle contraction (7, 15, 27, 38, 40).

However, ASM cells treated with each of the myosin inhibitors (W-7, ML-7, and BDM) did not show any sign of decrease in the F-actin polymerization induced by 5-HT and indicated, if anything, slightly increased actin polymerization (Fig. 6, *g–l*; Table 1). Each of these myosin inhibitors acts via a distinct mode of action to block the catalytic activity of myosin, and there were qualitative differences in response (Figs. 3–5). Cells treated with W-7, ML-7, or BDM all exhibited dose-dependent reductions of cell stiffening induced by 5-HT, but the relative potency of these inhibitors differed, with ML-7 being the most potent and BDM the least. In this connection, Katoh et al. (20) reported two different classes of stress fibers in cultured FS-133 cells, which are differentially regulated by myosin light chain kinase and Rho-kinase; central stress fibers are dependent on the activity of Rho-kinase, whereas peripheral stress fibers are dependent on the activity of myosin light chain kinase. Both ML-7 (25 μM) and W-7 (100 μM) inhibit formation of peripheral stress fibers in cultured FS-133 cells. In this study, we did not differentiate between the two classes of actin stress fibers but focused rather on the F-actin polymerization at the site near the dense plaques of ASM cells. Despite these differences in the myosin inhibitors and their mechanisms of action, the data in Figs. 3–6 draw a self-consistent picture in which the major part of the agonist-induced cell stiffening seems to be attributable to myosin activation. Each of these myosin inhibitors decreased baseline stiffness as well, suggesting that the baseline tone that these cells possess is attributable to partial myosin activation (16, 35).

To exert its mechanical effects, myosin must interact with an integrated actin lattice. Mehta and Gunst (27) reported that disrupting the actin lattice, either by capping existing actin filaments at the barbed ends with cytochalasin D or by preventing G-actin assembly

into actin filaments with latrunculin A, markedly depresses force development in response to contractile activation. Likewise, we found that inhibition of actin polymerization by 10 μM cytochalasin D or 1 μM latrunculin A completely ablated cell stiffening induced by 5-HT (Figs. 7 and 8). However, whereas a 1-h incubation with 1 μM cytochalasin D also blocked F-actin polymerization induced by 5-HT (Fig. 6, *d* and *e*; Table 1), this did not entirely ablate the cell stiffening response (Fig. 7). These findings seem to suggest that the partially disrupted actin CSK may still provide a scaffolding on which myosin motors can exert their mechanical effects.

Recent reports suggest that agonist-induced actin polymerization is mediated via pathways involving heterotrimeric G proteins $G\alpha_{i\text{-}2}$ and $G\alpha_q$ signaling to RhoA (15, 38). When passaged ASM cells were treated with C3 exoenzyme or Y-27632, the extent of cell stiffening induced by 5-HT was substantially attenuated (Figs. 9 and 10). These inhibitors at doses that completely blocked F-actin polymerization did not ablate the stiffening response to 5-HT, however. As regards the C3 exoenzyme data, we could not determine from these studies whether the observed attenuation of cell stiffness was due to incomplete inactivation of Rho or the presence of Rho-independent mechanisms for both actin polymerization and myosin light chain phosphorylation. Activation of RhoA and its downstream target Rho-kinase also has been shown to inactivate myosin light chain phosphatase (22). Although we did not measure the level of myosin light chain phosphorylation in these cells, our findings with a wide panel of F-actin inhibitors, together with findings of others (15, 27, 38, 40), seem to indicate that dynamic changes in the actin CSK and its attachment to the cell membrane may be an important component of the cell stiffening response to 5-HT. This leads us to the conclusion that agonist-evoked stiffening of cultured ASM cells requires actin polymerization as well as myosin activation and that neither process alone is sufficient to account for the observed cell stiffening.

As regards the role of myosin motors in changes of cell stiffness, there are at least three mechanisms that might contribute. The first mechanism is the direct effect of cross bridge recruitment. Huxley's 1957 (17) theory of muscle contraction shows that cross-linking of the thick filament to the thin filament by myosin bridges leads to changes of muscle stiffness in direct proportion to the number of bridges attached. This stiffness is attributable to the elasticity of the myosin S2 subfragment (18) and the extensibility of the thin and thick filaments themselves (28). A second plausible mechanism concerns an indirect effect of myosin activation, namely, the increased tension that is borne in filamentous structures of the CSK as a result of myosin activation. The tensegrity model suggests that cell stiffness is conferred by the tension borne by these filamentous structures. According to this hypothesis, as filament tension changes, the cell stiffness changes in concert, much as a simple tent becomes stiffer as its tethers are tightened (37, 42). Recent experimental data establish a linear relationship between cell stiffness and the tension generated within the CSK (43). In this case, changes of cell stiffness would be secondary to changes of filamentous tension caused by recruitment and activation of myosin bridges but not due to bridge stiffness itself.

The third myosin-based mechanism relates to the theory of myosin evanescence. It has been proposed that myosin filaments are structurally labile and that thick filaments may also undergo dynamic changes during contraction or relaxation of smooth muscle (23, 34). For example, contractile activation may provide a suitable environment for myosin to be incorporated into thick filaments, whereas muscle relaxation may promote thick filament depolymerization. Hence, the differences in cell stiffness may reflect the differences in the organization of myosin filaments after activation. These changes also confer ASM plasticity, which allows the cells to adapt to changes in muscle length as imposed by tidal breathing.

In summary, we have shown that 5-HT increases both cell stiffness and the formation of F-actin. Myosin inhibitors largely ablated the cell stiffening response but not the F-actin polymerization induced by 5-HT. Agents that inhibited the formation of F-actin attenuated both baseline stiffness and the extent of cell stiffening induced by 5-HT. The data in this report suggest that mechanical stiffening of cultured ASM cells that is induced by contractile activation requires both actin polymerization as well as myosin activation and that neither actin polymerization nor myosin activation by itself is sufficient to increase cell stiffness in response to a contractile agonist.

We thank Drs. Kathleen Morgan, Ning Wang, and Ben Fabry for their helpful comments.

This study was supported by National Heart, Lung, and Blood Institute Grants HL-07118, HL-33009, and HL-59682.

REFERENCES

1. **Barnes PJ.** Inflammatory mediator receptors and asthma. *Am Rev Respir Dis* 135: 526–531, 1987.
2. **Barron LA, Giardina JB, Granger JP, and Khalil RA.** High-salt diet enhances vascular reactivity in pregnant rats with normal and reduced uterine perfusion pressure. *Hypertension* 38: 730–735, 2001.
3. **Butler JP, Tolic-Nørrelykke IM, Fabry B, and Fredberg JJ.** Traction fields, moments, and strain energy that cells exert on their surroundings. *Am J Physiol Cell Physiol* 282: C595–C605, 2002.
4. **Chitano P, Wang J, Cox CM, Stephens NL, and Murphy TM.** Different ontogeny of rate of force generation and shortening velocity in guinea pig trachealis. *J Appl Physiol* 88: 1338–1345, 2000.
5. **Fabry B, Maksym GN, Shore SA, Moore PE, Panettieri RA Jr, Butler JP, and Fredberg JJ.** Time course and heterogeneity of contractile responses in cultured human airway smooth muscle cells. *J Appl Physiol* 91: 986–994, 2001.
6. **Fredberg JJ, Jones KA, Nathan M, Raboudi S, Prakash YS, Shore SA, Butler JP, and Sieck GC.** Friction in airway smooth muscle: mechanism, latch, and implications in asthma. *J Appl Physiol* 81: 2703–2712, 1996.
7. **Gerthoffer WT and Gunst SJ.** Focal adhesion and small heat shock proteins in the regulation of actin remodeling and contractility in smooth muscle. *J Appl Physiol* 91: 963–972, 2001.

8. **Gunst SJ.** Effect of length history on contractile behavior of canine tracheal smooth muscle. *Am J Physiol Cell Physiol* 250: C146–C154, 1986.
9. **Gunst SJ, Stropp JQ, and Flavahan NA.** Interaction of contractile responses in canine tracheal smooth muscle. *J Appl Physiol* 63: 514–520, 1987.
10. **Gunst SJ and Tang DD.** The contractile apparatus and mechanical properties of airway smooth muscle. *Eur Respir J* 15: 600–616, 2000.
11. **Hai CM and Murphy RA.** Regulation of shortening velocity by cross-bridge phosphorylation in smooth muscle. *Am J Physiol Cell Physiol* 255: C86–C94, 1988.
12. **Hai CM and Szeto B.** Agonist-induced myosin phosphorylation during isometric contraction and unloaded shortening in airway smooth muscle. *Am J Physiol Lung Cell Mol Physiol* 262: L53–L62, 1992.
13. **Halayko AJ, Camoretti-Mercado B, Forsythe SM, Vieira JE, Mitchell RW, Wylam ME, Hershenson MB, and Solway J.** Divergent differentiation paths in airway smooth muscle culture: induction of functionally contractile myocytes. *Am J Physiol Lung Cell Mol Physiol* 276: L197–L206, 1999.
14. **Halayko AJ and Solway J.** Molecular mechanisms of phenotypic plasticity in smooth muscle cells. *J Appl Physiol* 90: 358–368, 2001.
15. **Hirshman CA and Emala CW.** Actin reorganization in airway smooth muscle cells involves G_q and $G_{i\text{-}2}$ activation of Rho. *Am J Physiol Lung Cell Mol Physiol* 277: L653–L661, 1999.
16. **Hubmayr RD, Shore SA, Fredberg JJ, Planus E, Panettieri RA, Moller W, Heyder J, and Wang N.** Pharmacological activation changes stiffness of cultured human airway smooth muscle cells. *Am J Physiol Cell Physiol* 271: C1660–C1668, 1996.
17. **Huxley AF.** Muscle structure, and theories of contraction. *Prog Biophys Biophys Chem* 7: 255–318, 1957.
18. **Huxley AF and Simmons RM.** Proposed mechanism of force generation in striated muscle. *Nature* 233: 533–538, 1971.
19. **Kamm KE and Stull JT.** The function of myosin and myosin light chain kinase phosphorylation in smooth muscle. *Annu Rev Pharmacol Toxicol* 25: 593–620, 1985.
20. **Katoh K, Kano Y, Amano M, Kaibuchi K, and Fujiwara K.** Stress fiber organization regulated by MLCK and Rho-kinase in cultured human fibroblasts. *Am J Physiol Cell Physiol* 280: C1669–C1679, 2001.
21. **Katoh K, Kano Y, Masuda M, Onishi H, and Fujiwara K.** Isolation and contraction of the stress fibers. *Mol Biol Cell* 9: 1919–1938, 1998.
22. **Kimura K, Ito M, Amano M, Chihara K, Fukata Y, Nakafuku M, Yamamori B, Feng J, Nakano T, Okawa K, Iwamatsu A, and Kaibushi K.** Regulation of myosin phosphatase by Rho and Rho-associated kinase (Rho-kinase). *Science* 273: 245–248, 1996.
23. **Kuo KH, Wang L, Pare PD, Ford LE, and Seow CY.** Myosin thick filament lability induced by mechanical strain in airway smooth muscle. *J Appl Physiol* 90: 1811–1816, 2001.
24. **Laporte JD, Moore PE, Baraldo S, Jouvin MH, Church TL, Schwartzman IN, Panettieri RA Jr, Kinet JP, and Shore SA.** Direct effects of interleukin-13 on signaling pathways for physiological responses in cultured human airway smooth muscle cells. *Am J Respir Crit Care Med* 164: 141–148, 2001.
25. **Ma X, Wang Y, and Stephens NL.** Serum deprivation induces a unique hypercontractile phenotype of cultured smooth muscle cells. *Am J Physiol Cell Physiol* 274: C1206–C1214, 1998.
26. **Maksym GN, Fabry B, Butler JP, Navajas D, Tschumperlin DJ, Laporte JD, and Fredberg JJ.** Mechanical properties of cultured human airway smooth muscle cells from 0.05 to 0.4 Hz. *J Appl Physiol* 89: 1619–1632, 2000.
27. **Mehta D and Gunst SJ.** Actin polymerization stimulated by contractile activation regulates force development in canine tracheal smooth muscle. *J Physiol* 519.3: 829–840, 1999.
28. **Mijailovich SM, Fredberg JJ, and Butler JP.** On the theory of muscle contraction: filament extensibility and the development of isometric force and stiffness. *Biophys J* 71: 1475–1484, 1996.
29. **Moore PE, Laporte JD, Abraham JH, Schwartzman IN, Yandava CN, Silverman ES, Drazen JM, Wand MP, Panettieri RA Jr, and Shore SA.** Polymorphism of the beta(2)-adrenergic receptor gene and desensitization in human airway smooth muscle. *Am J Respir Crit Care Med* 162: 2117–2124, 2000.
30. **Panettieri RA, Murray RK, DePalo LR, Yadvish PA, and Kotlikoff IM.** A human airway smooth muscle cell line that retains physiological responsiveness. *Am J Physiol Cell Physiol* 256: C329–C335, 1989.
31. **Pauwels R, Van Der Straeten M, Weyne J, and Bazin H.** Genetic factors in non-specific bronchial reactivity in rats. *Eur J Respir Dis* 66: 98–104, 1985.
32. **Pavalko FM, Adam LP, Wu MF, Walker TL, and Gunst SJ.** Phosphorylation of dense-plaque proteins talin and paxillin during tracheal smooth muscle contraction. *Am J Physiol Cell Physiol* 268: C563–C571, 1995.
33. **Sanders-Bush E, Tsutsumi M, and Burris KD.** Serotonin receptors and phosphatidylinositol turnover. *Ann NY Acad Sci* 600: 224–235, 1990.
34. **Seow CY, Pratusevich VR, and Ford LE.** Series-to-parallel transition in the filament lattice of airway smooth muscle. *J Appl Physiol* 89: 869–876, 2000.
35. **Shore SA, Laporte J, Hall IP, Hardy E, and Panettieri RA Jr.** Effect of IL-1 beta on responses of cultured human airway smooth muscle cells to bronchodilator agonists. *Am J Respir Cell Mol Biol* 16: 702–712, 1997.
36. **Somlyo AP and Somlyo AV.** Signal transduction and regulation in smooth muscle. *Nature* 372: 231–236, 1994.
37. **Stamenovic D, Fredberg JJ, Wang N, Butler JP, and Ingber DE.** A microstructural approach to cytoskeletal mechanics based on tensegrity. *J Theor Biol* 181: 125–136, 1996.
38. **Togashi H, Emala CW, Hall IP, and Hirshman CA.** Carbachol-induced actin reorganization involves G_i activation of Rho in human airway smooth muscle cells. *Am J Physiol Lung Cell Mol Physiol* 274: L803–L809, 1998.
39. **Tolloczko B, Jia YL, and Martin JG.** Serotonin-evoked calcium transients in airway smooth muscle cells. *Am J Physiol Lung Cell Mol Physiol* 269: L234–L240, 1995.
40. **Tseng S, Kim R, Kim T, Morgan KG, and Hai CM.** F-actin disruption attenuates agonist-induced [Ca^{2+}], myosin phosphorylation, and force in smooth muscle. *Am J Physiol Cell Physiol* 272: C1960–C1967, 1997.
41. **Wang N, Butler JP, and Ingber DE.** Mechanotransduction across the cell surface and through the cytoskeleton. *Science* 260: 1124–1127, 1993.
42. **Wang N, Naruse K, Stamenovic D, Fredberg JJ, Mijailovich SM, Tolic-Nørrelykke IM, Polte T, Mannix R, and Ingber DE.** Mechanical behavior in living cells consistent with the tensegrity model. *Proc Natl Acad Sci USA* 98: 7765–7770, 2001.
43. **Wang N, Tolic-Nørrelykke IM, Chen J, Mijailovich SM, Butler JP, Fredberg JJ, and Stamenovic D.** Cell prestress. I. Stiffness and prestress are closely associated in adherent contractile cells. *Am J Physiol Cell Physiol* 282: C606–C616, 2002.
44. **Wang Z, Pavalko FM, and Gunst SJ.** Tyrosine phosphorylation of the dense plaque protein paxillin is regulated during smooth muscle contraction. *Am J Physiol Cell Physiol* 271: C1594–C1602, 1996.
45. **Warshaw DM, Rees DD, and Fay FS.** Characterization of cross-bridge elasticity and kinetics of cross-bridge cycling force development in single smooth muscle cells. *J Gen Physiol* 91: 761–779, 1988.
46. **Wong JZ, Woodcock-Mitchell J, Mitchell J, Rippetoe P, White S, Absher M, Baldor L, Evans J, Mchugh KM, and Low RB.** Smooth muscle actin and myosin expression in cultured airway smooth muscle cells. *Am J Physiol Lung Cell Mol Physiol* 274: L786–L792, 1998.